Electronic Supplementary Material (ESI) for Physical Chemistry Chemical Physics.

Supporting Information

A Quantitative Methodology for the Study of Particle-Electrode Impacts

Christopher A. Little, ‡ Ruochen Xie, ‡ Christopher Batchelor-McAuley, Enno Kätelhön, Xiuting Li, Neil P. Young and Richard G. Compton*

* corresponding author: Richard G. Compton, Department of Chemistry, Physical & Theoretical Chemistry Laboratory, Oxford University, South Parks Road, Oxford, OX1 3QZ, United Kingdom

‡ C.A.L. and R.X. contributed equally

Email: richard.compton@chem.ox.ac.uk. Tel: +44(0)1865275 957 Fax: +44(0)1865275410

Contents

S1: TEM images of silver nanoparticles

The silver nanoparticles were imaged by transmission electron microscopy (TEM) using a JEOL JEM-3000F instrument with an accelerating voltage of 300 kV. Samples were prepared by drop casting nanoparticle suspensions (48 pM AgNPs, 2 mM sodium citrate) onto carbon grids (Agar Scientific) and allowing these to dry. Image extraction was subsequently performed using ImageJ software.

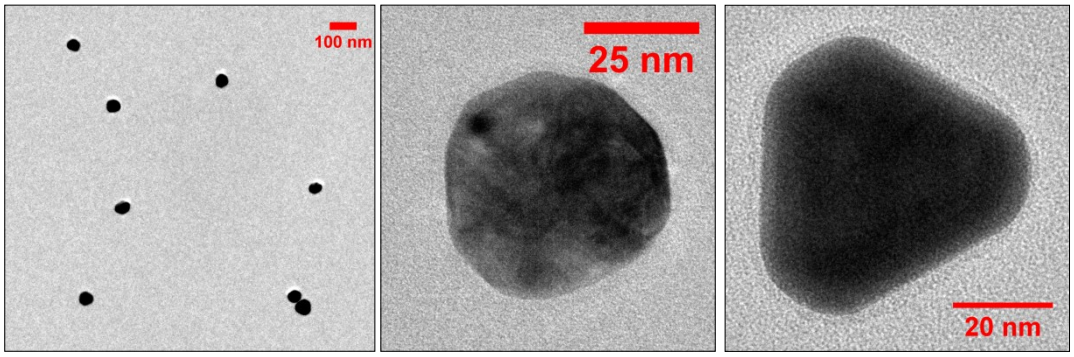

Figure S1. Representative TEM images of commercial spherical citrate-capped silver nanoparticles of 50 nm diameter (NanoXact, 0.02 mg mL^{-1}, 2 mM sodium citrate)

S2: Flow diagram of experimental measurement system

The flow diagram in Figure S2 depicts the key stages of the data acquisition process during a nano-impact experiment. Initially the working electrode is held at a virtual ground by the current amplifier, giving a low impedance pathway for the signal (a). The amplifier serves to both amplify the signal and convert it to a voltage (at a conversion of 1 GV/A), this amplification is done with bandwidth of 4 kHz, where the transfer function of the device closely approximates a first-order filter response. Then the voltage signal output of the amplifier is further filtered to 2 kHz using two cascaded passive RC filters (b). Following this, the filtered voltage signal is digitised by the data-acquisition device at a rate of 100 kS s^{-1} (c). Also of importance is the input resolution of the DAQ- in the present case a 16-bit device has been used. The device subsequently sends the digitised signal via a USB connection to the computer. Next, the computer receives and stores the digitised data (d), and this data can be loaded and analysed. If desired, it can be filtered prior to this using a digital low-pass filter, which limits the signals bandwidth (e).

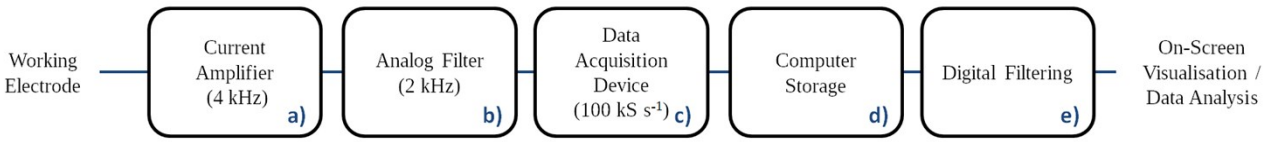

Figure S2. Flow diagram outlining the used measurement and filtering procedure for nano-impact experiments.

S3: Details of baseline estimation methodology

In order to analyse the electrochemical spike data an estimation of the baseline needs to be made. This may be done by an individual user on a per spike basis i.e. by manually selecting the 'start' and 'end' of a spike and assuming the background varies approximately linearly over the course of the event. Alternatively, more automated techniques for spike detection may be sought. A problem here lays in the large and relatively slowly changing experimental background signal. This leaves the development of such automated methodologies facing a number of complexities. In the present work the duration of a spike is defined by the points at which the current passes through this pre-defined baseline. Consequently, accurate estimation of the background is paramount to the validity of the analysis carried out. Automated spike identification has a propensity to underestimate the charge per event and requires validation against other analysis procedures prior to being employed.

The method utilised in this work briefly is outlined as follows:

Prior to estimation of the baseline, areas of the time trace containing impact events require removal. In this work we achieve this through analysing the local windowed variance. Using an adapted version of the Welford's method for a one pass calculation of a datasets variance, the rolling windowed standard deviation can be rapidly estimated with a high degree of accuracy. Having calculated the windowed regions of high variance likely to correspond to times at which a nano-event is occurring, data windows with a variance above a set threshold are removed from the data set. The threshold is set by the user as a percentile across the whole dataset with values between 70 and 95% are commonly employed. In order to estimate the baseline the regions where data has been removed is filled by an estimate of the baseline. Note, simply filling the formed gaps in the dataset by linear interpolation is found to be insufficient in providing an accurate baseline estimate. Having filled the data gaps, the resulting dataset with the 'spikes' removed is digitally filtered to a very low frequency using a 4-pole Bessel filter (ca. 5 Hz). Note a two pass filtering is used first in the forward and then in the reverse direction to avoid phase shifting the resulting baseline. The final filtered response is used as the baseline for the spike detection algorithm. It should be noted that although the baseline estimation and spike identification is semi-automated, the developed script forces the user to validate the baseline and analysis of each individual spike prior to its use in the final data set.

S4: Charge distributions using a windowing method

One method of obtaining a charge distribution is to measure data in its raw format, without applying a digital filter, and then clustering spikes together that occur within a given time window. In this case, if the current crosses the baseline more than once within a certain time window these multiple peaks will count as a single event, with the charge calculated by integrating over the whole range of these spikes. Figure S4a depicts the cumulative frequency charge distributions obtained for suspensions of 12 pM AgNPs in 20 mM KCl over three chronoamperograms using this method. Window sizes from 0 ms to 50 ms are used, and the data filtered at 100 Hz overlaid. It can be seen that a window size of 15 ms is in excellent agreement with the data filtered at 100 Hz, except at low charge (< 0.2 pC).

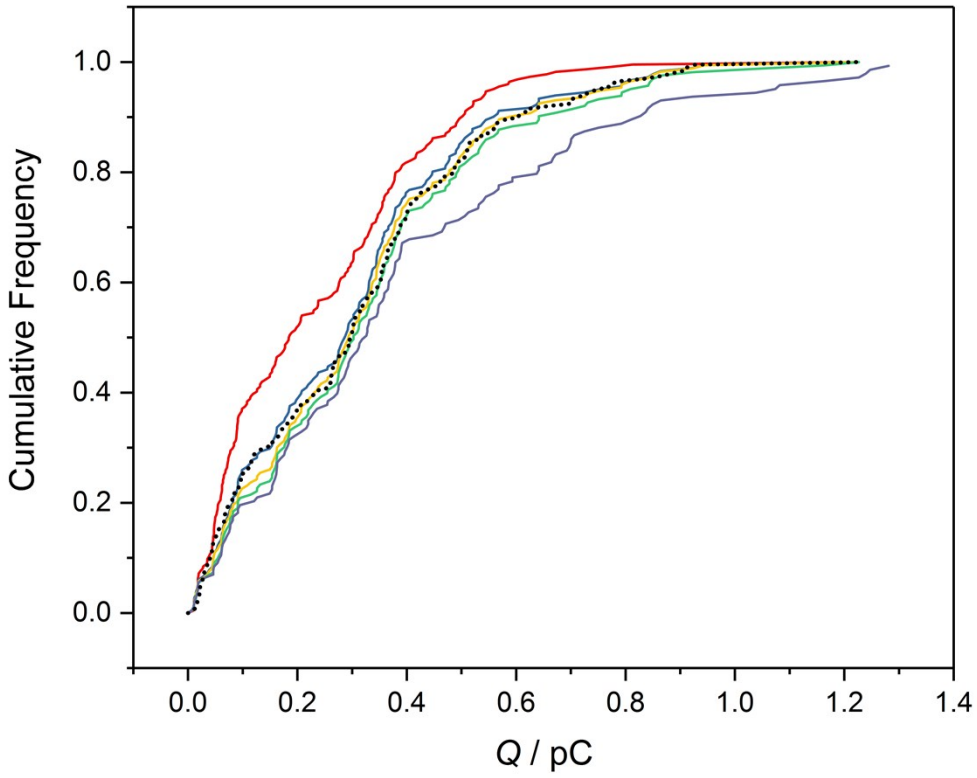

Figure S4a. Cumulative frequency plots of the charge transferred during nano-impacts of 12 pM AgNPs in 20 mM KCl for three chronoamperograms. The data was obtained by detecting spikes from the raw, unfiltered data and then clustering spikes based on a window size. Window sizes of 0 ms, 10 ms, 15 ms, 20 ms and 50 ms are depicted as red, blue, yellow, green and purple solid lines respectively. Overlaid is the same charge distribution obtained from digitally filtering the data at 100 Hz prior to analysis (dotted black line).

As referenced in the main text, by using the high frequency raw data recorded at 2 kHz and clustering the spikes into events based on a 15 ms window size, the average spike charge is underestimated by approximately 5 %. Whilst the overall percentage error is relatively small in magnitude, the error

associated with individual spike events can be as high as 70 %. This data is presented in Figure S4b, with Figure S4bi depicting the correlation between 149 spikes measured by the two methods, excluding 21 'vanishing' spikes and 5 spikes that are split into doublets using the window-size method. Figure S4bii demonstrates that whilst there is a fairly small percentage change at higher charges (> 0.5 pC), the more extreme disparity comes with lower charge impacts; 10 % of the spike population show a 50 % or greater decrease in charge from the 100 Hz to window-size methods, and all of these are for spikes of magnitudes lower than 0.3 pC.

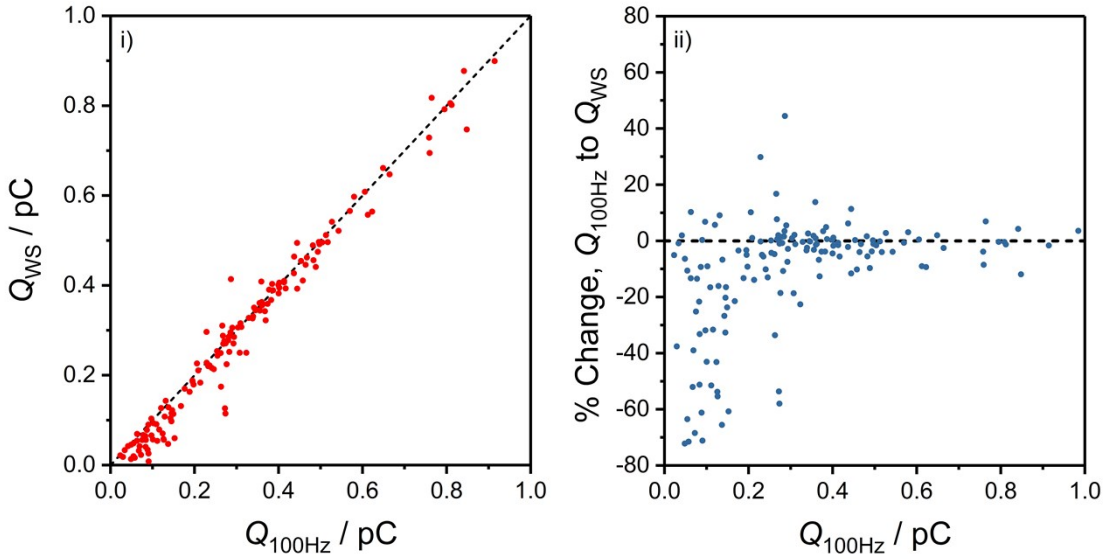

Figure S4b. i) Correlation diagrams for the charge of nano-impact spikes measured with a post-acquisition 100 Hz digital filter applied (Q_{100Hz}) compared to the charge measured by detecting spike events in the raw data, and clustering them together based on a 15 ms window size (Q_{WS}). ii) Scatter plot showing the percentage change in measured charge from the method involving a post-acquisition 100 Hz digital filter applied (Q_{100Hz}) to the window-sizing method (Q_{WS}), plotted against the measured charge at 100 Hz.

S5: Correction factors used in TEM

Without the use of tomography or other 3D techniques, attempting to obtain nanoparticle volume distributions from TEM images requires significant assumptions and approximations regarding the geometry of the particles. The TEM images in Figure S5a depict the variation in shapes observed for this batch of silver nanoparticles, with the heterogeneity of the morphology clearly evident.

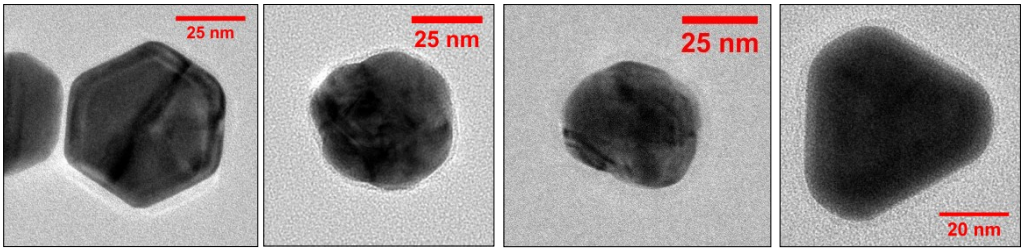

Figure S5a. Representative TEM images showing the variability in dimension and morphology of nominally 50 nm diameter AgNPs.

As referenced in the main text, the estimation of the nanoparticle volume distribution and hence oxidative charge distribution must take into account a correction factor for their non-sphericity. The charge distribution presented in Figure 7 of the main text was constructed by calculating the volume of the nanoparticles as given in Equation 1:

$$V_{NP} = \frac{4\pi {R_s}^3}{3} \times f \quad (1)$$

where R_s is the radius of the sphere circumscribing the nanoparticle, and is taken to be the maximal radius for non-spherical particles (approximately 50 % of the sample). The value of f is taken to be 1 for spherical particles, and has previously been chosen semi-arbitrarily to be 0.5 for non-spherical particles.[1] Assuming complete oxidation of the nanoparticle, the charge transferred per nanoparticle Q_{NP} can then be calculated as given in Equation 2:

$$Q_{NP} = \frac{\rho z F}{A_r} \times V_{NP} \quad (2)$$

where ρ is the density of silver (10.5×10^6 g m^{-3}),[2] z is the number of electrons transferred per atom (equal to 1 for silver oxidation), and A_r is the atomic mass of silver (107.9 g mol^{-1}).

Due to the large proportion of non-spherical particles in this sample, the choice of correction factor f can have a significant impact on the shape and mean of the charge distribution obtained from the TEM images. As a result, we have presented the distributions resulting from the range of correction factors 0.5 - 0.7, demonstrating the influence of f, and further highlighting the difficulties in using the circularity of a 2D projection to provide a good volume estimate.

References

1. Ngamchuea, K.; Clark, R. O. D.; Sokolov, S. V.; Young, N. P.; Batchelor‐McAuley, C.; Compton, R. G., Single Oxidative Collision Events of Silver Nanoparticles: Understanding the Rate‐Determining Chemistry. *Chemistry-A European Journal* **2017,** *23* (63), 16085-16096.
2. Weast, R. C., *CRC Handbook of Chemistry and Physics: 1974-1975 (55th ed.)*. CRC Press: 1974.